Hypoglycosylated E-cadherin promotes the assembly of tight junctions through the recruitment of PP2A to adherens junctions

Mihai Nita-Lazar[1], **Ivan Rebustini**[2], **Janice Walker**[3], and **Maria A. Kukuruzinska**[1,#]

[1]Department of Molecular and Cell Biology, Boston University Medical Center, Boston, MA 02118
[2]Matrix and Morphogenesis Unit, Craniofacial Developmental Biology and Regeneration Branch, National Institute for Dental and Craniofacial Research, National Institutes of Health, Bethesda, Maryland [3]Department of Pathology, Anatomy and Cell Biology, Thomas Jefferson University, Philadelphia, Pennsylvania

Abstract

Epithelial cell-cell adhesion is controlled by multiprotein complexes that include E-cadherin-mediated adherens junctions (AJs) and ZO-1-containing tight junctions (TJs). Previously, we reported that reduction of E-cadherin N-glycosylation in normal and cancer cells promoted stabilization of AJs through changes in the composition and cytoskeletal association of E-cadherin scaffolds. Here, we show that enhanced interaction of hypoglycosylated E-cadherin-containing AJs with protein phosphatase 2A (PP2A) represents a mechanism for promoting TJ assembly. In MDCK cells, attenuation of cellular N-glycosylation with siRNA to DPAGT1, the first gene in the N-glycosylation pathway, reduced N-glycosylation of surface E-cadherin and resulted in increased recruitment of stabilizing proteins γ-catenin, α-catenin, vinculin and PP2A to AJs. Greater association of PP2A with AJs correlated with diminished binding of PP2A to ZO-1 and claudin-1 and with increased pools of serine-phosphorylated ZO-1 and claudin-1. More ZO-1 was found in complexes with occludin and claudin-1, and this corresponded to enhanced transepithelial resistance (TER), indicating physiological assembly of TJs. Similar maturation of AJs and TJs was detected after transfection of MDCK cells with the hypoglycosylated E-cadherin variant, V13. Our data indicate that E-cadherin N-glycans coordinate the maturity of AJs with the assembly of TJs by affecting the association of PP2A with these junctional complexes.

Keywords

adherens junctions; E-cadherin N-glycosylation; PP2A; tight junctions

Introduction

Epithelial tissues achieve their mature organization and function, in part, through the formation of stable junctions between adjacent cells [1–4]. These include adherens junctions (AJs), which mediate adhesion between cells, and tight junctions (TJs), which are responsible for the barrier

function of epithelia [5–7]. Each of the intercellular junctional complexes is a dynamic structure that comprises numerous proteins and undergoes changes in composition depending on cell and/or tissue context [6].

In epithelial cells, the principal component of AJs is E-cadherin, a calcium-dependent N-glycoprotein adhesion receptor [1,5,8]. In the presence of calcium, the extracellular segments of E-cadherin dimerize and interact with E-cadherin dimers on adjacent cells [9]. These extracellular contacts are stabilized through the interaction of E-cadherin cytoplasmic regions with catenins [10,11]. Both β-catenin- and γ-catenin bind to E-cadherin's cytoplasmic tail in a mutually exclusive manner and recruit α-catenin. Although the molecular details of α-catenin function are unclear, its association with E-cadherin-catenin complexes leads to the reorganization of the actin cytoskeleton and promotes adhesion [12,13]. E-cadherin-catenin complexes interact with actin crosslinking, scaffolding and signaling proteins, through which they regulate diverse cell functions including cell proliferation, survival and differentiation [2,14–16]. Recent studies have shown that in addition to the actin cytoskeleton, E-cadherin junctions interact with microtubules (MTs), and that this tethering of AJs to MTs plays a role in the stabilization of cell-cell adhesion [17,18].

Among proteins shown to be important for the maintenance of AJs is protein phosphatase 2A (PP2A). PP2A is a serine/threonine protein phosphatase that forms a hetero-trimeric complex containing catalytic (C), scaffold (A) and regulatory (B) subunits. PP2A plays critical roles in cell growth, signaling and tumor suppression [19,20] and its activity is controlled, in part, by the interaction of different proteins with its catalytic subunit, PP2A-C. Mouse blastocysts lacking the PP2A catalytic subunit, PP2A-C, have disorganized cell mass with E-cadherin being redistributed from the cell borders to the cytosol [21]. In non-malignant human mammary epithelial cells, inhibition of PP2A results in internalization of E-cadherin-catenin complexes [22]. Furthermore, loss of PP2A from AJs has been recently correlated with cellular discohesion in oral squamous cell carcinoma [23].

In contrast to its stabilizing effect on AJs, PP2A has been shown to negatively regulate the biogenesis of TJs [24]. TJs assemble apically from AJs as a set of continuous intramembranous particle strands that create a paracellular permeability barrier and separate the apical plasma membrane from the basolateral domain in polarized epithelia [7,25]. TJs are composed of transmembrane proteins including claudins and occludin that are linked to the actin cytoskeleton via intracellular plaque proteins ZO-1 and ZO-2. Claudins constitute the backbone of TJ strands and are essential for the size and ion specificity of the TJ barrier while ZO-1 and ZO-2 determine the sites of TJ assembly [26].

Formation of E-cadherin junctions has been shown to precede the establishment of TJs. Early in cell-cell contact formation, E-cadherin-catenin complexes recruit ZO-1 to the primordial cell-cell adhesion sites [27–30]. Upon AJ stabilization, ZO-1 redistributes apically to the sites of prospective TJs where it functions as a scaffold protein and recruits claudins and occludin. In the developing murine epidermis, E-cadherin is required for the formation of TJs *in vivo* because its deficiency results in the mislocalization of key tight junctional components, leading to transepithelial water loss and perinatal death [31].

Our previous studies have shown that modification of E-cadherin ectodomains (ECs) 4 and 5 with N-glycans impacts the composition and stability of E-cadherin scaffolds. In particular, removal of complex N-glycans from EC 4 promotes the association of E-cadherin with γ-catenin and vinculin and enhances their interaction with the actin cytoskeleton [32]. Likewise, hypoglycosylated E-cadherin interacts more readily with dynein and PP2A, thus promoting the interaction of AJs with MTs. N-glycosylation of E-cadherin is physiologically significant because it is subject to changes with cell density [32,33] and epithelial phenotype development

[34]. In sparse Madin-Darby canine kidney (MDCK) cells lacking mature AJs, E-cadherin is primarily N-glycosylated with complex oligosaccharides, while E-cadherin N-glycosylation is greatly reduced in dense cultures with stable junctional complexes [32,33]. Our most recent studies have shown that hyperglycosylation of E-cadherin in oral cancer cells is associated with the destabilization of AJs and TJs, cellular discohesion and tumor spread [23].

N-glycosylation status of proteins is regulated by the level of expression of the DPAGT1 gene encoding dolichol-P-dependent N-acetylglucosamine-1-phosphate-transferase [35–37]. Evolutionarily conserved and essential for viability, DPAGT1 initiates the synthesis of the lipid-linked oligosaccharide (LLO) precursor for protein N-glycosylation in the endoplasmic reticulum (ER) [38–41]. On a mechanistic level, DPAGT1 expression determines the amount of LLO and, therefore, the extent of protein N-glycosylation [35,36]. DPAGT1 is regulated with growth; it displays abundant expression in proliferating cells that is diminished in dense cultures [42,43]. Thus, N-glycosylation status of E-cadherin is directly related to the level of DPAGT1 expression.

Because the formation of AJs precedes TJ assembly, and because E-cadherin N-glycans destabilize AJs, we examined whether E-cadherin N-glycans affected the organization and function of TJs. In the present study, we show that partial inhibition of DPAGT1 in MDCK cells led to reduced N-glycosylation of E-cadherin, stabilization of AJs, enhancement of TJs, increased cell compaction and diminished proliferation. Similar results were obtained with MDCK cells transfected with the hypoglycosylated E-cadherin variant, V13 [32], indicating that intracellular adhesion was driven by diminished N-glycosylation of E-cadherin. On a mechanistic level, increased interaction of hypoglycosylated E-cadherin complexes with PP2A resulted in reduced association of PP2A with ZO-1 and claudin-1. This promoted the formation of ZO-1-occludin-claudin-1 complexes concomitant with an increase in transepithelial resistance (TER). Collectively, our studies provide evidence that E-cadherin N-glycans inhibit intercellular adhesion by excluding PP2A from AJs and facilitating its association with TJs.

Materials and Methods

Reagents and antibodies

Polyclonal antibody to the conserved 11 amino acid C-terminal sequence of DPAGT1 was prepared commercially (Covance). Monoclonal antibody to the cytoplasmic region of human E-cadherin, as well as monoclonal antibodies to α-catenin, β-catenin, γ-catenin, PP2A-C, ZO-1 and IgG isotype controls were obtained from BD Transduction Laboratories. Monoclonal antibody to gp135 (hybridoma supernatant, 3F2) was a gift from George Ojakian (SUNY Downstate Medical Center, Brooklyn, NY). Monoclonal antibodies to the myc tag and vinculin (clone V284) were from Cell Signaling and Upstate Biotechnology, respectively. Monoclonal antibody to actin (pan Ab-5, clone ACTN05) was from NeoMarkers. Polyclonal antibodies to occludin and claudin-1 were from Zymed. Antibodies to calnexin were obtained from Abcam. Rhodamine-phalloidin was obtained from Molecular Probes. Secondary antibodies included goat anti-mouse or anti-rabbit IgG derivatized with either fluorescein isothiocyanate or Alexa Fluor (Molecular Probes). Horseradish peroxidase-conjugated secondary antibodies were from Amersham Biosciences. Protein G Sepharose and Protein A Agarose beads were purchased from Sigma. Trypan blue was obtained from Cambrex BioScience and the EZ-Link Sulfo-NHS-SS-Biotin and Immobilized Streptavidin were from Pierce. FLAG antibody was obtained from BD.

Cell culture, transfections and preparation of cell lysates

MDCK cells were from American Type Culture Collection. MDCK cells were maintained in DMEM (Gibco) supplemented with 10% FBS, penicillin and streptomycin. To partially inhibit

DPAGT1 expression, MDCK cells were transfected at 50% confluence with DPAGT1 siRNA and with a non-silencing control using Lipofectamine 2000 (Invitrogen) and grown for 72 h. MDCK cells were also transfected with cDNAs encoding E-cadherin and its N-glycosylation variant V13 using Lipofectamine 2000 and enriched for exogenous E-cadherins with 0.8 µg/µl G418 for two weeks. For preparation of cell lysates, MDCK cells, either treated with siRNA to DPAGT1 or transfected with wild type E-cadherin and V13, were extracted with 600 µ l of ice-cold Triton X-100/β-octylglucosidase buffer (10 mM imidazole, 100 mM NaCl, 1 mM MgCl$_2$, 5 mM Na$_2$EDTA, 1% Triton X-100, 0.87 mg/ml β-octylglucosidase) containing 50 µg/ml aprotinin, 25 µg/ml soybean trypsin inhibitor, 100 µM benzamidine, 5 µg/ml leupeptin and 0.5 µM PMSF. Protein concentrations were determined by using BCA protein assay (Pierce).

siRNA treatment

siRNA targeting DPAGT1 were obtained as a SMART-pool™ sequences from Dharmacon. Non-silencing negative control siRNA was purchased from Qiagen. The efficiency of transfections was determined using off-target Cy3-siRNA (Dharmacon).

Quantitative RT-PCR

Total RNAs were isolated from MDCK cells transfected either with DPAGT1 siRNA or non-silencing control and used for cDNA synthesis to assess DPAGT1 gene expression by real-time PCR. The gene expression profiles were generated by normalizing the Ct (threshold cycle numbers) of DPAGT1 with a housekeeping gene S29 and comparing the gene expression of cells treated with non-silencing and silencing DPAGT1 siRNAs using three concentrations of siRNAs (40 nM, 60 nM and 80 nM). Statistical analysis was performed using real-time PCR from three independent RNA preparations, with each experiment being repeated twice (n = 6). The *P* value between the non-silencing and silencing siRNA treatments for DPAGT1 expression was calculated using unpaired *t*-test statistical analysis.

E-cadherin N-glycosylation variant V13

A PCR-based site-directed mutagenesis of human E-cadherin gene was carried out using primers for the replacement of asparagine (Asn) for glutamine (Gln) in the N-glycosylation sites Asn404 > Gln and Asn483 > Gln with a QuickChange XL Site Directed Mutagenesis Kit (Stratagene) as described before [32].

Cell viability

MDCK cells were seeded in six-well plates at a density of 1.3×10^4 cells/cm^2, grown to 50% confluence and transfected with either DPAGT1 siRNA or non-silencing control. Cells were grown for 72 h, harvested by trypsinization and viability was assessed by the trypan blue exclusion assay [44,45].

Surface biotinylation

MDCK cells, transfected with either DPAGT1 siRNA or non-silencing control, were surface biotinylated using Sulfo-NHS-LC-Biotin according to manufacturer's instructions (Pierce). Biotinylated transfectants were extracted with the lysis buffer, biotin-labeled protein fraction was isolated with streptavidin agarose beads and the surface labeled E-cadherin was detected by Western blot using an antibody that recognizes its cytoplasmic domain.

Deglycosylation of E-cadherin

Total cell lysates and biotin-labeled E-cadherins were digested with 100 U of PNGaseF and/ or EndoH (New England Biolabs) for 1h at 37°C and analyzed by Western blot. For controls, samples were incubated without the enzymes.

Western blot

Total cell lysates, 10 µg of protein, were fractionated on 7.5% SDS-PAGE and blotted onto nitrocellulose membranes (Invitrogen). The samples were blocked with 10% milk, and membranes were incubated with primary antibodies at appropriate dilutions in PBS-Tween (20 mM Tris/137 mM NaCl/ 0.1% Tween 20, pH 7.6) with 1% milk for 2 h at room temperature (RT). Next, membranes were washed four times with PBS-Tween, followed by incubation with horseradish peroxidase-linked secondary antibody (1:3000). The results were visualized with ECL Plus Detection Reagents (Amersham Biosciences). Error bars represent standard deviation from three independent experiments; *P*-values were calculated by unpaired two-tailed *t*-test.

Immunoprecipitation

Equal amounts of total cell lysate (200 µ g) were precleared with IgG isotype control antibodies and 30 µl of protein G-coupled Sepharose beads or protein A-coupled Agarose beads, incubated for 2 h at 4°C with 2.5 µg of antibodies against either E-cadherin or ZO-1 followed by incubation with protein G or A beads. The beads were washed three times with the lysis buffer (10 mM Tris HCl pH 7.5, 1 mM EDTA, 1 mM EGTA and 0.5% Triton X-100), samples were resuspended in 100 µl of 2X SDS sample buffer, boiled for 5 min at 95°C and analyzed by Western blot.

Flow cytometry

MDCK cells, transfected with wild type E-cadherin and with the V13 N-glycosylation variant, or with siRNA to DPAGT1, were collected by centrifugation. The cells were resuspended in 1 ml of PBS at RT, then transferred to 4 ml of absolute ethanol and placed at −20°C for 5–15 minutes, after which they were resuspended in 5 ml of PBS for 15 minutes. Next, the cells were treated with ribonuclease (1mg/ml) for 5 minutes at RT and resuspended in 200 µl of 3 µM PI solution. Analyses were performed with FACScan (Becton Dickinson) and CellQuest Pro software.

Transepithelial resistance

Cells were seeded onto Transwells (polycarbonate membrane, 12-mm diameter, 0.4 µm pore size; Corning Costar), grown to confluence and TER was measured directly in culture media using an epithelial voltohmmeter (World Precision Instruments). To assess the effects of DPAGT1 siRNA on TER, MDCK cells were plated at 5×10^4 cells per cm^2, grown to ~50% confluence and transfected with either DPAGT1 or non-silencing siRNAs, as described above. Transfectants were then grown for an additional 72 h to establish confluent monolayers. MDCK cells, transfected with either wild type E-cadherin or its V13 variant, were plated at 1.5×10^5 cells per cm^2 and grown for 48–72 h to confluence. TER was measured keeping constant distances from the bottom of the well and between the electrodes. Values were calculated after subtracting background readings from blank Transwells with the medium, cultured in parallel. Data were analyzed by unpaired two-tailed *t*-test. Error bars represent standard deviation from three independent experiments.

Microscopy, immunofluorescence and imaging

Morphological analyses were conducted with epifluorescence Nikon Eclipse TE300 microscope. For indirect immunofluorescence analyses, cells were fixed in 3.7% paraformaldehyde, permeabilized with 0.1% Triton X-100, blocked with 10% goat serum and incubated with primary antibodies to either E-cadherin (0.25 µg/ml), the myc tag (0.25 µg/ml), ZO-1 (0.25 µg/ml), claudin-1 (0.25 µg/ml) or gp135 (hybridoma supernatant, 3F2, 1:100) overnight at 4°C. Cells were then incubated with FITC-tagged secondary antibodies (0.1 µg/ml) and, when indicated, were counterstained with rhodamine-phalloidin (1:100). The immunostained samples were analyzed with a Zeiss confocal laser scanning microscope LSM510 META (Fluar 5X/0.25, magnification Plan-Apochromat 40X/1.3 oil DIC). For visualization of individual optical sections and for generation of Z-stacks with optical slices of 0.74 µm, LSM510-expert mode acquisition software was used. To ensure valid comparison of fluorescence intensities between samples, settings were fixed to the most highly stained sample and all other images were acquired at those settings.

Results

Partial inhibition of DPAGT1 with siRNA leads to reduced N-glycosylation of E-cadherin and remodeling of AJs

Previous studies have shown that the N-glycosylation status of E-cadherin is reduced in dense cultures coincident with the formation of stable AJs [32–34]. Since the expression of DPAGT1, which initiates the synthesis of the LLO precursor for protein N-glycosylation and regulates the extent of protein N-glycosylation, is also downregulated with cell density [35,43], we hypothesized that DPAGT1 was a determinant of E-cadherin N-glycosylation status. Thus, we sought to partially inhibit DPAGT1 expression using siRNA, to an extent that occurs *in vivo* under growth arrest and differentiation, with the goal of reducing E-cadherin N-glycosylation. Concentrations of DPAGT1 siRNA ranging from 40 nM to 60 nM caused a dose-dependent inhibition of DPAGT1 mRNA expression by 20% and 35%, respectively, as determined by quantitative RT-PCR (Fig. 1A). Under these conditions, the efficiency of transfection, measured by the uptake of Cy3 siRNA, was 98%. No deleterious effects on cell viability were detected, as determined by the trypan blue exclusion assay (Fig. 1A). Inhibition of DPAGT1 transcript levels by 35% with 60 nM siRNA corresponded to a 40% reduction in its protein levels (Fig. 1B). In contrast, treatment of cells with 80 nM siRNA led to a greater than 80% inhibition in DPAGT1 mRNA levels and 60% loss of cell viability (Fig. 1A). The nonlinear reduction in DPAGT1 transcript levels in response to progressive increases in siRNA may reflect differences in the effective concentrations of siRNA in the micelles. We note that 30% – 40 % downregulation in DPAGT1 expression occurs under normal physiological conditions that accompany growth arrest and differentiation [43]. As expected, diminished DPAGT1 expression did not affect the expression of a resident ER protein calnexin (CNX), a protein chaperone that recognizes inappropriately N-glycosylated proteins and functions in the UPR (Fig. 1C) [46,47]. Similarly, no change in CNX expression was detected after transfection of MDCK cells with the hypoglycosylated N-glycosylated E-cadherin variant, V13 (Fig. 1D). Since treatment with 60 nM siRNA caused the reduction of 35% and 40% in DPAGT1 transcript and protein abundance, respectively, without affecting cell viability, this siRNA concentration was used in all subsequent studies.

Immunoblot analyses revealed that E-cadherin from cells transfected with a non-silencing control siRNA migrated with a higher molecular size compared to E-cadherin from DPAGT1 siRNA-treated cells (Fig. 2A lanes 1 and 4). This suggests that partial inhibition of DPAGT1 expression caused reduction of E-cadherin N-glycosylation status. We further assessed E-cadherin N-glycosylation using sensitivities to EndoH and PNGaseF. EndoH is an endoglycosidase that cleaves high mannose and hybrid N-glycans at the chitobiose core, while

PNGaseF is an amidase that removes most N-glycans. Based on the mobility shifts before and after EndoH and PNGaseF treatments, E-cadherin from non-silenced cells was modified with both high mannose/hybrid and complex oligosaccharides (Fig. 2A, NS, lanes 2 and 3). In contrast, E-cadherin from silenced cultures displayed similar sensitivities to EndoH and PNGaseF, indicating that it contained mostly high mannose/hybrid N-glycans (Fig. 2A, S lanes 5 and 6). We conclude that partial inhibition of DPAGT1 effectively reduced E-cadherin N-glycosylation status with complex N-glycans. This result confirmed our previous studies, showing that removal of the major complex N-glycans from EC4 led to stablilization of AJs [32]. Moreover, this was consistent with the reported virtual absence of complex N-glycans on N-cadherin in late cultures of clone-YH cells [34] and on desmosomal cadherins in the mature epidermis [48]. In contrast, a recent study found diminished N-glycosylation of E-cadherin in dense cultures to correlate with reduced branching of complex N-glycans but not with their absence *per se* [33].

Similar levels of E-cadherin expression were found in total cell lysates (TCLs) from non-silenced and silenced cells after normalization to actin (Fig 2B, TCL). To determine if diminished N-glycosylation status affected the localization of E-cadherin, we labeled the surface pools of E-cadherin in non-silenced and silenced cells with biotin and analyzed them by Western blot. Biotinylated pools of E-cadherin from non-silenced and silenced cells were found comparable in abundance (Fig. 2C), and biotinylated E-cadherin from silenced cells migrated with a lower molecular weight than from non-silenced cells (Fig. 2C). Moreover, treatment of biotinylated E-cadherins from both non-silenced and silenced cells with EndoH and PNGaseF produced changes in mobility similar to those observed with respective TCLs (Figs. 2A and 2D). Hence, 60 nM DPAGT1 siRNA reduced N-glycosylation of surface E-cadherin.

Phase contrast imaging showed that partial silencing of DPAGT1 and reduced E-cadherin N-glycosylation correlated with increased cell compaction, with non-silenced cells numbering 39 and silenced cells numbering 68 per 100 μm^2 within their respective islands (Fig. 3A, NS and S). This was not due to increased proliferation of silenced cells, because silenced cells exhibited slower growth as indicated by their longer doubling times (Fig. 3B). Also, flow cytometry analysis of asynchronous cultures revealed an increased number of silenced cells in the G1 phase of the cell cycle compared to non-silenced cells (Table 1, S versus NS).

Previously, we showed that diminished N-glycosylation of E-cadherin resulted in increased recruitment of γ-catenin and vinculin to E-cadherin scaffolds [32]. Downregulation of cellular N-glycosylation with siRNA to DPAGT1 did not affect the expression of several proteins known to be associated with E-cadherin or with its scaffolds (Fig. 3C). Under these conditions, immunoprecipitation with IgG isotype control did not reveal any non-specific interactons with E-cadherin protein complexes (Fig. 3D). Thus, E-cadherin-containing AJs in silenced cells were more mature compared to non-silenced cells. To determine whether attenuation of E-cadherin N-glycosylation with DPAGT1 siRNA led to similar remodeling of AJs, we examined E-cadherin complexes from non-silenced and silenced cells. When E-cadherin immunoprecipitates were analyzed for associated proteins by immunoblot, E-cadherin complexes from silenced cells exhibited an increased abundance of γ-catenin, α-catenin and vinculin compared to non-silenced cells (Fig. 3E).

Our recent studies have also provided evidence that hypoglycosylated E-cadherin preferentially interacted with PP2A [18], supporting the requirement for reduced N-glycosylation in the stabilization of intercellular adhesion [21,22]. Therefore, we also tested E-cadherin immunoprecipitates from DPAGT1-inhibited cells for association with the catalytic subunit of PP2A, PP2A-C. E-cadherin complexes from silenced cells exhibited a three-fold increase in the amount of PP2A-C compared to non-silenced cultures (Fig. 3F). We were unable

to detect significant differences in the association of PP2A with the transfected exogenous E-cadherins in MDCK cells using an antibody to the myc tag (data not shown). This could be due to the limiting amount of PP2A, as well as the likelihood that the endogenous E-cadherin competed for and sequestered PP2A, since at the time of harvest the endogenous E-cadherin would have reduced N-glycosylation status.

Because E-cadherin junctions are stabilized through the recruitment and bundling of actin filaments at the sites of AJs, we next evaluated the distribution of E-cadherin and filamentous actin (F-actin) by fluorescence staining. Indirect immunofluorescence localization of E-cadherin using an antibody to its cytoplasmic region and staining for F-actin with rhodamine-phalloidin showed that in silenced cells, E-cadherin was well organized at cell-cell borders where it co-localized with F-actin (Fig. 3G).

Increased cell compaction was also characteristic of MDCK cells transfected with the hypoglycosylated E-cadherin variant, V13, reflecting 56 cells per μm^2 compared to wild type E-cadherin or 35 cells per μm^2 in their respective islands (Fig. 4A). Similar to silenced cells, this was not due to increased proliferation, as V13 transfectants displayed longer doubling times (Fig. 4B) and had more cells in the G1 phase of the cell cycle (Table 1, E-cad versus V13), consistent with the stabilization of AJs by V13. As expected, the hypoglycosylated E-cadherin variant, V13, also exhibited a two-fold increased interaction with PP2A compared to wild type E-cadherin in MDCK cells (Fig. 4C).

Confocal imaging confirmed that in V13 transfectants, E-cadherin displayed co-localization with F-actin at cell-cell borders similar to cells with wild type E-cadherin (Fig. 4D). We note that, for immunofuorescence localization, wild type and V13 E-cadherins were detected with an antibody to the myc tag to distinguish between exogenous and endogenous E-cadherins [32]. Collectively, these data show that DPAGT1 siRNA affected cell morphology and E-cadherin distribution in a manner similar to the hypoglycosylated V13 variant.

Hypoglycosylated E-cadherin inhibits association of PP2A with ZO-1 and claudin-1 and drives TJ assembly

In contrast to its role in the maintenance of AJs, association of PP2A with the components of TJs has been shown to inhibit their phosphorylation and organization into functional junctions [24]. Since reduced E-cadherin N-glycosylation status promoted the maturation of AJs, we predicted that ZO-1 complexes from silenced cells should have less E-cadherin and PP2A than nonsilenced cells. Western blot analyses of TJ components revealed that DPAGT1 siRNA did not affect the expression of ZO-1, occludin or claudin-1 (Fig. 5A). Next, we examined ZO-1-containing protein complexes in non-silenced and silenced cells under the immunoprecipitation condition in which the IgG isotype control did not reveal non-specific interactions with ZO-1 protein complexes (Fig. 5B). In non-silenced cells, there was substantially more ZO-1 in complex with E-cadherin scaffolds (Fig. 5C), shown to mark immature or primordial AJs [28]. This finding was confirmed by reverse immunoprecipitation with E-cadherin (Fig. 5D).

Importantly, ZO-1 scaffolds in silenced cells contained more occludin and claudin-1 compared to non-silenced cells, but less PP2A, an inhibitor of TJ assembly (Fig. 5E). Similarly, claudin-1 exhibited diminished association with PP2A in silenced cells (Fig. 5G). The latter finding correlated with increased phosphorylation status of ZO-1 (Fig. 5F) and claudin-1 (Fig. 5H). These results showed that hypoglycosylated E-cadherin promoted the remodeling of TJs by attenuating their association with PP2A and thus driving phosphorylation of ZO-1 and claudin-1. Indirect immunofluorescence of ZO-1 and claudin-1 revealed that these tight junction components were well organized at cell-cell borders in silenced cells (Fig. 5I). However, based on the immunolocalization pattern of gp135, an apical membrane marker,

silenced cells had more prominent apical domains compared to non-silenced cells (Fig. 5J, gp135, *x–z*) and more pronounced apical lateral localization of ZO-1 (Fig. 5J, ZO-1, *x–z*).

Increases in both, the association of ZO-1 with claudin-1 and occludin and in the phosphorylation of ZO-1 and claudin-1 in silenced cells coincident with a more apical localization of ZO-1 suggested that reduced N-glycosylation of E-cadherin favored the formation of functional TJs. Therefore, we next compared the integrity of TJs in non-silenced and silenced cells by measuring TER. In MDCK cells, TER has been shown to be a direct indicator of tightness of the paracellular seal and a measure of paracellular permeability [49]. Confluent non-silenced cell monolayers formed TJs that displayed a steady-state TER of 265 Ohm-cm^2, while silenced cell monolayers formed TJs that maintained a higher TER of 341 Ohm-cm^2 (Fig. 5K). These results show that partial inhibition of N-glycosylation caused an increase in MDCK cell TER.

To confirm that E-cadherin N-glycosylation status was responsible for the remodeling of TJs, we compared the composition of TJs in MDCK cells transfected with either wild type E-cadherin or its hypoglycosylated variant, V13. In cells transfected with wild type E-cadherin, ZO-1 complexes had less claudin-1 but more PP2A than in V13-transfected cells (Fig. 6A). Also, claudin-1 was found to be associated with reduced levels of PP2A in V13-tranfected cells (Fig. 6C). Diminished association with PP2A correlated with increased phosphorylation status of ZO-1 (Fig. 6B) and claudin-1 (Fig. 6D). These results show that, similar to DPAGT1 siRNA, the hypoglycosylated E-cadherin variant, V13, promoted the remodeling of TJs by attenuating their association with PP2A and allowing phosphorylation of ZO-1 and claudin-1. Indirect immunofluorescence analyses confirmed that ZO-1 localized to cell-cell borders in V13-transfected cells (Fig. 6E). Similar to silenced cells, V13-transfected cells exhibited a more pronounced localization of gp135 at the apical domains (Fig. 6F, gp135, *x–z*) and of ZO-1 at the apical lateral borders (Fig. 6F, ZO-1, *x–z*). Measurements of the functional integrity of TJs by TER in monolayers of cells transfected with either wild type E-cadherin or V13 showed that V13-myc-transfectants formed TJs that maintained a higher TER compared to the wild type E-cadherin- transfected cells (Fig. 6G). Therefore, these data indicate that hypoglycosylated E-cadherin enhanced the integrity of TJs.

Discussion

E-cadherin junctions comprise dynamic multiprotein ensembles whose components either directly or indirectly regulate AJs stability. Formation of AJs has been linked to the assembly of TJs, although the molecular details of this relationship have been unclear. The present study provides insights into the interplay between AJs and TJs and shows that hypoglycosylation of E-cadherin drives the recruitment of PP2A to AJs through which it promotes the assembly of TJs.

We have employed downregulation of N-glycosylation as an experimental strategy to elucidate the mechanism via which E-cadherin N-glycans affect intercellular adhesion. Partial inhibition of DPAGT1 protein abundance diminished N-glycosylation of surface E-cadherin without affecting cell viability or expression of an ER resident protein chaperone calnexin (Fig. 1 and Fig. 2). Because DPAGT1 regulates the synthesis of the lipid-linked oligosaccharide precursor and the extent of protein N-glycosylation, its reduced expression had to affect the N-glycosylation status of *de novo* synthesized E-cadherin. The time course required for siRNA to diminish DPAGT1 protein levels and to reduce N-glycosylation of E-cadherin resembled the kinetics of AJ maturation in cultured MDCK cells [32,33]. This was different from Ca^{+2} switch experiments that typically use confluent cells that synthesize only hypoglycosylated E-cadherin [50,51].

Our data show that the N-glycosylation status of E-cadherin is a determinant of its adhesive function. Diminished N-glycosylation of E-cadherin did not interfere with its targeting to the cell surface (Fig. 2), but rather led to the remodeling and stabilization of AJs. Specifically, hypoglycosylated E-cadherin preferentially bound γ-catenin. This initial E-cadherin/γ-catenin complex had a higher affinity for interacting with α-catenin at the sites of AJs. While α-catenin monomers interact with E-cadherin-β/γ-catenin, α-catenin dimers regulate the bundling of actin filaments [12]. This suggests that preferential recruitment of α-catenin to E-cadherin/γ-catenin complexes promoted interaction with the actin cytoskeleton. Indeed, hypoglycosylated E-cadherin/γ-catenin/α-catenin complexes exhibited increased association with vinculin. Interaction of vinculin with F-actin has been suggested to collaborate with α-catenin to promote vinculin activation and formation of actin bundles [52]. Hypoglycosylated E-cadherin also associated more with PP2A (Fig. 3F and Fig. 4C), which has been shown to be required for AJ function [22]. We have recently reported that one role of this preferential recruitment of PP2A to hypoglycosylated E-cadherin-containing AJs was to enhance the tethering of AJs to MTs, which may promote transport of polarity proteins to the apical domains of cells forming mature AJs [18].

A novel finding of the present work is the evidence that increased recruitment of PP2A to AJs containing hypoglycosylated E-cadherin correlated with enhanced assembly of TJs. PP2A is a negative regulator of TJ assembly, because it prevents phosphorylation of ZO-1, occludin and claudin-1 and inhibits the activity of aPKC [24]. Indeed, increased interaction of PP2A with AJs containing hypoglycosylated E-cadherin coincided with diminished association between PP2A and TJ components, ZO-1 and claudin-1, and with their increased phosphorylation status (Fig. 5F, G and Fig. 6B, C). This correlated with a greater interaction between ZO-1 and claudin-1. Furthermore, changes in the molecular organization of TJs were physiologically significant as reflected by an increase in monolayer TER. Reduced association of PP2A with TJs and its increased association with AJs suggested that, in addition to the presence of PP2A in the cytosol, there was a pool of PP2A that shuttled between tight junctional components and AJs [53]. Although E-cadherin has been shown to be critical for TJ assembly [31], the novel finding of our studies is that not only the presence of E-cadherin, but also its reduced N-glycosylation status, plays a critical role in promoting intercellular adhesion. Consistent with increased recruitment of stabilizing components to AJs and enhanced assembly of TJs, cells with hypoglycosylated E-cadherin displayed greater compaction and reduced proliferation (Fig. 3 and Fig. 4). Lastly, E-cadherin-mediated cell-cell contacts have been mechanistically linked to the initiation of polarity through the interaction of AJs with basolateral proteins specified by the Exocyst and the lateral SNARE complex [54]. Since both silenced cells and V13-transfected cells exhibited better definition of apical domains, this suggested that through the enhancement of cell-cell adhesion, hypoglycosylated E-cadherin promoted cell polarity. Future studies evaluating interactions of hypoglycosylated E-cadherin with basolateral proteins, such as aquaporin3, will provide support for this notion.

Interestingly, our data show that extensively N-glycosylated E-cadherin appears to maintain AJs in their nascent state. Early in cell-cell contact formation, a pool of ZO-1 interacts with E-cadherin/β-catenin/α-catenin complexes and forms primordial junctions [27,28]. Such primordial junctions comprise extensively N-glycosylated E-cadherin, since little ZO-1 was found in complexes with hypoglycosylated E-cadherin. We also note that under conditions of extensive N-glycosylation of E-cadherin, another pool of ZO-1 interacted with PP2A, which was likely responsible for its dephosphorylated state.

Thus, the mechanism through which E-cadherin N-glycans regulate intercellular adhesion involves changes in the composition and cytoskeletal association of E-cadherin scaffolds. Hypoglycosylated E-cadherin complexes appear to organize larger scaffolds with increased stoichiometries of stabilizing proteins. It is possible that by virtue of having fewer and/or

smaller complex N-glycans, the extracellular domains of hypoglycosylated E-cadherin form stronger bonds *in trans* that result in a conformational change of its cytoplasmic domain. This may lead to an increased association with α-catenin, vinculin and PP2A, as well as with cytoskeletal components. Increased association of hypoglycosylated E-cadherin-containing AJs with PP2A may be responsible for removing PP2A-mediated inhibition of ZO-1 and claudin-1, thus promoting TJ assembly. Since PP2A has been shown to protect E-cadherin from endocytosis [55], increased interaction with PP2A may also play a role in the maintenance of hypoglycosylated E-cadherin at the cell surface.

In addition to E-cadherin, attenuation of cellular N-glycosylation with DPAGT1 had to affect N-glycosylation status of other proteins involved in intercellular adhesion. While none of the components of TJs are N-glycosylated, nectins and Na^+,K^+-ATPase represent glycoproteins that impact AJ stability [33,56]. Similar to Na^+, K^+-ATPase and E-cadherin, nectins are likely to be stabilized by reduced N-glycosylation and N-glycan complexity [32,33]. Another intercellular junction shown to have interdependence with AJs is the desmosome [57]. In the mature epidermis, desmosomal cadherins are modified primarily with high mannose N-glycans [48], suggesting that diminished N-glycosylation is associated with stable desmosome structures. Here, our results support a recent report showing that diminished modification of surface proteins, including E-cadherin and Na^+,K^+-ATPase, with highly branched complex N-glycans promoted intracellular adhesion [33]. We show, however, that the enhancement of TJ assembly is specific to E-cadherin N-glycans because the hypoglycosylated E-cadherin variant V13 alone could drive molecular reorganization of AJs and TJs and augment TER.

The present study reveals a novel and physiologically significant mechanism through which the metabolic pathway of protein N-glycosylation impacts intercellular adhesion. This mechanism is also likely to be valid in tumorigenesis, where unwarranted increases in cellular N-glycosylation destabilize AJs and drive disassembly of TJs [23,58]. A model of how E-cadherin N-glycans affect intracellular junctions is shown in Fig. 7. We propose that one target of E-cadherin's N-glycans is PP2A, which coordinates the activities of intercellular adhesion complexes so that in the presence of nascent AJs cells do not assemble TJs, but upon maturation of AJs they organize TJs and seal the epithelia.

Abbreviations

AJs	adherens junctions
CHO	Chinese Hamster Ovary
CNX	calnexin
ECs	E-cadherin ectodomains
ER	endoplasmic reticulum
F-actin	filamentous actin
MDCK	Madin-Darby canine kidney
PP2A	protein phosphatase 2A
TCL	total cell lysate
TER	transepithelial resistance
TJs	tight junctions
UPR	unfolded protein response

Acknowledgments

References

1. Hirano S, Nose A, Hatta K, Kawakami A, Takeichi M. Calcium-dependent cell-cell adhesion molecules (cadherins): specificities and possible involvement of actin bundles. J. Cell Biol 1987;105:2501–2511. [PubMed: 3320048]

2. Jamora C, Fuchs E. Intercellular adhesion, signalling and the cytoskeleton. Nat. Cell Biol 2002;4:101–108.

3. Larue L, Ohsugi M, Hirchenhain J, Kemler R. E-cadherin null mutant embryos fail to form a trophectoderm epithelium. Proc. Natl. Acad. Sci. USA 1994;91:8263–8267. [PubMed: 8058792]

4. Gumbiner BM. Cell adhesion: the molecular basis of tissue architercture and morphogenesis. Cell 1996;84:345–357. [PubMed: 8608588]

5. Gumbiner B, Stevenson B, Grimaldi A. The role of the cell adhesion molecule uvomorulin in the formation and maintenance of the epithelial junctional complex. J. Cell Biol 1988;107:1575–1587. [PubMed: 3049625]

6. Niessen CM. Tight junctions/adherens junctions: basic structure and function. J Invest Dermatol 2007;127:2525–2532. [PubMed: 17934504]

7. Matter K, Aijaz S, Tsapara A, Balda MS. Mammalian tight junctions in the regulation of epithelial differentiation and proliferation. Curr. Opin. Cell Biol 2005;17:453–458. [PubMed: 16098725]

8. Wheelock MJ, Johnson KR. Cadherins as modulators of cellular phenotype. Ann. Rev. Cell Dev. Biol 2003;19:207–235. [PubMed: 14570569]

9. Yap AS, Briecher WM, Pruschy M, Gumbiner BM. Lateral clustering of the adhesive ectodomain: a fundamental determinant of cadherin function. Curr. Biol 1997;7:308–315. [PubMed: 9133345]

10. Nathke IS, Hinck L, Nelson WJ. The cadherin/catenin complex: connections to multiple cellular processes involved in cell adhesion, proliferation and morphogenesis. Sem. Dev. Biol 1995;6:89–95.

11. Gumbiner BM. Regulation of cadherin adhesive activity. J. Cell Biol 2000;148:399–404. [PubMed: 10662767]

12. Drees F, Pokutta S, Yamada S, Nelson WJ, Weis WI. Alpha-catenin is a molecular switch that binds E-cadherin-beta-catenin and regulates actin filament assembly. Cell 2005;123:903–915. [PubMed: 16325583]

13. Yamada S, Pokutta S, Drees F, Weis WI, Nelson WJ. Deconstructing the cadherin-catenin-actin complex. Cell 2005;123:889–901. [PubMed: 16325582]

14. Wheelock MJ, Johnson KR. Cadherin-mediated cellular signaling. Curr. Opin. Cell Biol 2003;15:509–514. [PubMed: 14519384]

15. Perez-Moreno M, Jamora C, Fuchs E. Sticky business: orchestrating cellular signals at adherens junctions. Cell 2003;112:535–548. [PubMed: 12600316]

16. Liu WF, Nelson CM, Pirone DM, Chen CS. E-cadherin engagement stimulates proliferation via Rac1. J. Cell Biol 2006;173:431–441. [PubMed: 16682529]

17. Stehbens SJ, Paterson AD, Crampton MS, Shewan AM, Ferguson C, Akhmanova A, Parton RG, Yap AS. Dynamic microtubules regulate the local concentration of E-cadherin at cell-cell contacts. Journal of Cell Science 2006;119:1801–1811. [PubMed: 16608875]

18. Jamal BT, Nita-Lazar M, Gao Z, Amin B, Walker J, Kukuruzinska MA. N-glycosylation status of E-cadherin controls cytoskeletal dynamics through the organization of distinct b-catenin and g-catenin-containing AJs. Cell Health Cytoskeleton 2009;1:67–80.

19. Sontag E. Protein phosphatase 2A: the trojan horse of cellular signaling. Cell Signal 2001;13:7–16. [PubMed: 11257442]

20. Janssens V, Goris J. Protein phosphatase 2A: a highly regulated family of serine/threonine phosphatases implicated in cell growth and signaling. Biochem. J 2001;353:417–439. [PubMed: 11171037]

21. Gotz J, Probst A, Mistl C, Nitsch RM, Ehler E. Distinct role of protein phosphatase 2A subunit Cα in the regulation of E-cadherin and β-catenin during development. Mech. Dev 2000;93:83–93. [PubMed: 10781942]

22. Takahashi K, Nakajima E, Suzuki K. Involvement of protein phosphatase 2A in the maintenance of E-cadherin-mediated cell-cell adhesion through recruitment of IQGAP1. J. Cell. Physiol 2006;206:814–820. [PubMed: 16245300]

23. Nita-Lazar M, Noonan V, Rebustini I, Walker J, Menko AS, Kukuruzinska MA. Overexpression of DPAGT1 leads to aberrant N-glycosylation of E-cadherin and cellular discohesion in oral cancer. Cancer Res 2009;69:5673–5680. [PubMed: 19549906]

24. Nunbhakdi-Craig V, Machleidt T, Ogris E, Bellotto D, White CL III, Sontag E. Protein phosphatase 2A associates with and regulates atypical PKC and the epithelial tight junction complex. J. Cell Biol 2002;158:967–978. [PubMed: 12196510]

25. Shin K, Fogg VC, Margolis B. Tight junctions and cell polarity. Annu. Rev. Cell Dev. Biol 2006;22:207–235. [PubMed: 16771626]

26. Umeda K, Ikenouchi J, Katahira-Tayama S, Furuse K, Sasaki H, Nakayama M, Matsui T, Tsukita S, Furuse M, Tsukita S. ZO-1 and ZO-2 independently determine where claudins are polymerized in tight-junction strand formation. Cell 2006;126:741–754. [PubMed: 16923393]

27. Suzuki A, Ishiyama C, Hashiba K, Shimizu M, Ebnet K, Ohno S. aPKC kinase activity is required for the asymmetric differentiation of the premature junctional complex during epithelial cell polarization. J. Cell Sci 2002;115:3565–3573. [PubMed: 12186943]

28. Rajasekaran AK, Hojo M, Huima T, Rodriguez-Boulan E. Catenins and zonula occludens-1 form a complex during early stages in the assembly of tight junctions. J. Cell Biol 1996;132:451–463. [PubMed: 8636221]

29. Muller SL, Portwich M, Schmidt A, Utepbergenov DI, Huber O, Blasig IE, Krause G. The tight junction protein occludin and the adherens junction protein α-catenin share a common interaction mechanism with ZO-1. J. Biol. Chem 2005;280:3747–3756. [PubMed: 15548514]

30. Itoh M, Nagafuchi A, Moroi S, Tsukita S. Involvement of ZO-1 in cadherin-based cell adhesio through its direct binding to alpha catenin and actin filaments. J. Cell Biol 1997;138:181–192. [PubMed: 9214391]

31. Tunggal JA, Helfrich I, Schmitz A, Schwarz H, Gunzel D, Fromm M, Kemler R, Krieg T, Niessen CM. E-cadherin is essential for in vivo epidermal barrier function by regulating tight junctions. EMBO J 2005;24:1146–1156. [PubMed: 15775979]

32. Liwosz A, Lei T, Kukuruzinska MA. N-glycosylation affects the molecular organization and stability of E-cadherin junctions. J. Biol. Chem 2006;281:23138–23149. [PubMed: 16682414]

33. Vagin O, Tokhtaeva E, Yakubov I, Shevchenko E, Sachs G. Inverse Correlation between the Extent of N-Glycan Branching and Intercellular Adhesion in Epithelia: CONTRIBUTION OF THE Na,K-ATPase 1 SUBUNIT. J Biol Chem 2008;283:2192–2202. [PubMed: 18025087]

34. Youn YH, Hong J, Burke JM. Cell phenotype in normal epithelial cell lines with high endogenous N-cadherin: comparison of RPE to an MDCK subclone. Invest Ophthalmol Vis Sci 2006;47:2675–2685. [PubMed: 16723486]

35. Mendelsohn RD, Helmerhorst E, Cipollo JF, Kukuruzinska MA. A hypomorphic allele of the first N-glycosylation gene, ALG7, causes mitochondrial defects in yeast. Biochim. Biophys. Acta 2005;1723:33–44. [PubMed: 15794922]

36. Wu X, Rush JS, Karaoglu D, Krasnewich D, Lubinsky MS, Waechter CJ, Gilmore R, Freeze HH. Deficiency of UDP-GlcNAc:Dolichol Phosphate N-Acetylglucosamine-1 Phosphate Transferase (DPAGT1) causes a novel congenital disorder of Glycosylation Type Ij. Hum Mutat 2003;22:144–150. [PubMed: 12872255]

37. Kukuruzinska MA, Apekin V, Lamkin MS, Hiltz A, Rodriguez A, Lin CC, Paz MA, Oppenhein FG. Antisense RNA to the first N-glycosylation gene, ALG7, inhibits protein N-glycosylation and secretion by Xenopus oocytes. Biochem. Biophys. Res. Comm 1994;198:1248–1254. [PubMed: 7509600]

38. Kukuruzinska MA, Robbins PW. Protein glycosylation in yeast: transcript heterogeneity of the ALG7 gene. Proc. Natl. Acad. Sci. USA 1987;84:2145–2149. [PubMed: 3031666]

39. Marek KW, Vijay IK, Marth JD. A recessive deletion in the GlcNAc-1-phosphotransferase gene results in peri-implantation embryonic lethality. Glycobiol 1999;9:1263–1271.

40. Kornfeld S, Kornfeld R. Assembly of asparagine-linked oligosaccharides. Ann. Rev. Biochem 1985;54:631–664. [PubMed: 3896128]

41. Kukuruzinska MA, Bergh MLE, Jackson BJ. Protein glycosylation in yeast. Ann. Rev. Biochem 1987;56:631–664.

42. Kukuruzinska MA, Lennon-Hopkins K. ALG gene expression and cell cycle progression. Biochem. Biophys. Acta 1999;1426:359–372. [PubMed: 9878828]

43. Fernandes RP, Cotanche DA, Lennon-Hopkins K, Erkan F, Menko AS, Kukuruzinska MA. Differential expression of proliferative, cytoskeletal, and adhesive proteins during postnatal development of the hamster submandibular gland. Histochem. Cell Biol 1999;111:153–162. [PubMed: 10090576]

44. Mesner PW, Winters TR, Green SH. Nerve growth factor withdrawal-induced cell death in neuronal PC12 cells resembles that in sympathetic neurons. J. Cell Biol 1992;119:1669–1680. [PubMed: 1469055]

45. Zhou S, Baltimore D, Cantley LC, Kaplan DR, Franke TF. Interleukin 3-dependent survival by the Akt protein kinase. Proc. Natl. Acad. Sci. USA 1997;94:11345–11350. [PubMed: 9326612]

46. Schroder M, Kaufman RJ. The mammalian unfolded protein response. Annu. Rev. Biochem 2005;74:739–789. [PubMed: 15952902]

47. Parodi AJ. Protein glucosylation and its role in protein folding. Annu. Rev. Biochem 2000;69:69–93. [PubMed: 10966453]

48. Uematsu R, Furukawa J, Nakagawa H, Shinohara Y, Deguchi K, Monde K, Nishimura S. High throughput quantitative glycomics and glycoform-focused proteomics of murine dermis and epidermis. Mol Cell Proteomics 2005;4:1977–1989. [PubMed: 16170054]

49. Matter K, Balda MS. Functional analysis of tight junctions. Methods 2003;30:228–234. [PubMed: 12798137]

50. Cereijido M, Shoshani L, Contreras RG. Molecular physiology and pathophysiology of tight junctions. I. Biogenesis of tight junctions and epithelial polarity. Am J Physiol Gastrointest Liver Physiol 2000;279:G477–G482. [PubMed: 10960345]

51. Straight SW, Pieczynski JN, Whiteman EL, Liu CJ, Margolis B. Mammalian lin-7 stabilizes polarity protein complexes. J Biol Chem 2006;281:37738–37747. [PubMed: 17012742]

52. Janssen ME, Kim E, Liu H, Fujimoto LM, Bobkov A, Volkmann N, Hanein D. Three-dimensional structure of vinculin bound to actin filaments. Mol Cell 2006;21:271–281. [PubMed: 16427016]

53. Sontag E. Protein phosphatase 2A: the Trojan Horse of cellular signaling. Cellular Signalling 2001;13:7–16. [PubMed: 11257442]

54. Nejsum LN, Nelson WJ. A molecular mechanism directly linking E-cadherin adhesion to initiation of epithelial cell surface polarity. J Cell Biol 2007;178:323–335. [PubMed: 17635938]

55. Suzuki K, Takahashi K. Induction of E-cadherin endocytosis by loss of protein phosphatase 2A expression in human breast cancers. Biochem Biophys Res Commun 2006;349:255–260. [PubMed: 16930554]

56. Miyoshi J, Takai Y. Nectin and nectin-like molecules: biology and pathology. Am J Nephrol 2007;27:590–604. [PubMed: 17823505]

57. Yin T, Green KJ. Regulation of desmosome assembly and adhesion. Semin Cell Dev Biol 2004;15:665–677. [PubMed: 15561586]

58. Dennis JW, Granovsky M, Warren CE. Glycoprotein glycosylation and cancer progression. Biochim. Biophys. Acta 1999;1473:21–34. [PubMed: 10580127]
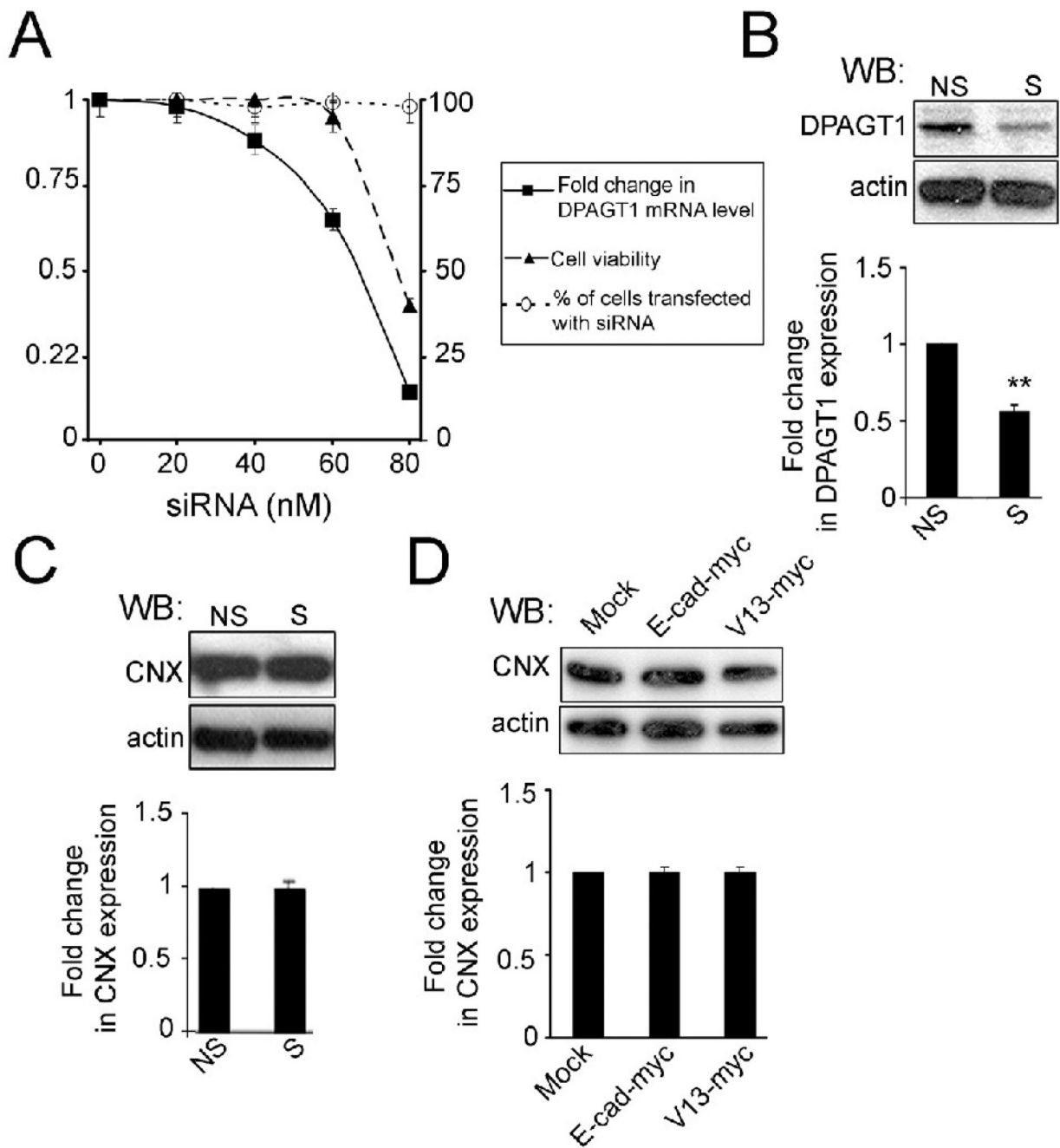
Fig. 1.
Silencing of DPAGT1 in MDCK cells. (A), Graph displaying the effects of different concentrations of DPAGT1 siRNA on DPAGT1 transcript levels (filled squares) and cell viability (filled triangles). Cy3-siRNA was used to determine transfection efficiency (open circles). Shown are means +/− S.E. from three independent experiments. (B), DPAGT1 protein levels following transfection with 60 nM siRNA. Total cell lysates (TCLs) from MDCK cells transfected with non-silencing (NS) and DPAGT1 (S) siRNAs were analyzed for DPAGT1 protein levels by Western blot (WB). Fold change of DPAGT1 abundance in silenced (S) cells was determined in comparison with non-silenced (NS) cells after normalization to actin. Data were obtained from three different experiments (**P<0.01). (C), TCLs from non-silenced (NS)

and silenced (S) cells were examined for CNX expression by WB with an anti-CNX antibody. Fold change of CNX protein levels from silenced (S) cells was determined in comparison with non-silenced (NS) cells after normalization to actin using data from three independent experiments (**P<0.01). (D), TCLs from cells transiently transfected with either wild-type E-cadherin (E-cad-myc), V13 (V13-myc) or the empty plasmid (Mock) were analyzed for CNX expression by WB with an anti-CNX antibody. Fold changes of CNX protein levels from E-cad-myc- and V13-myc-transfected cells were determined in comparison with mock-transfected cells after normalization to actin using data from three different experiments.
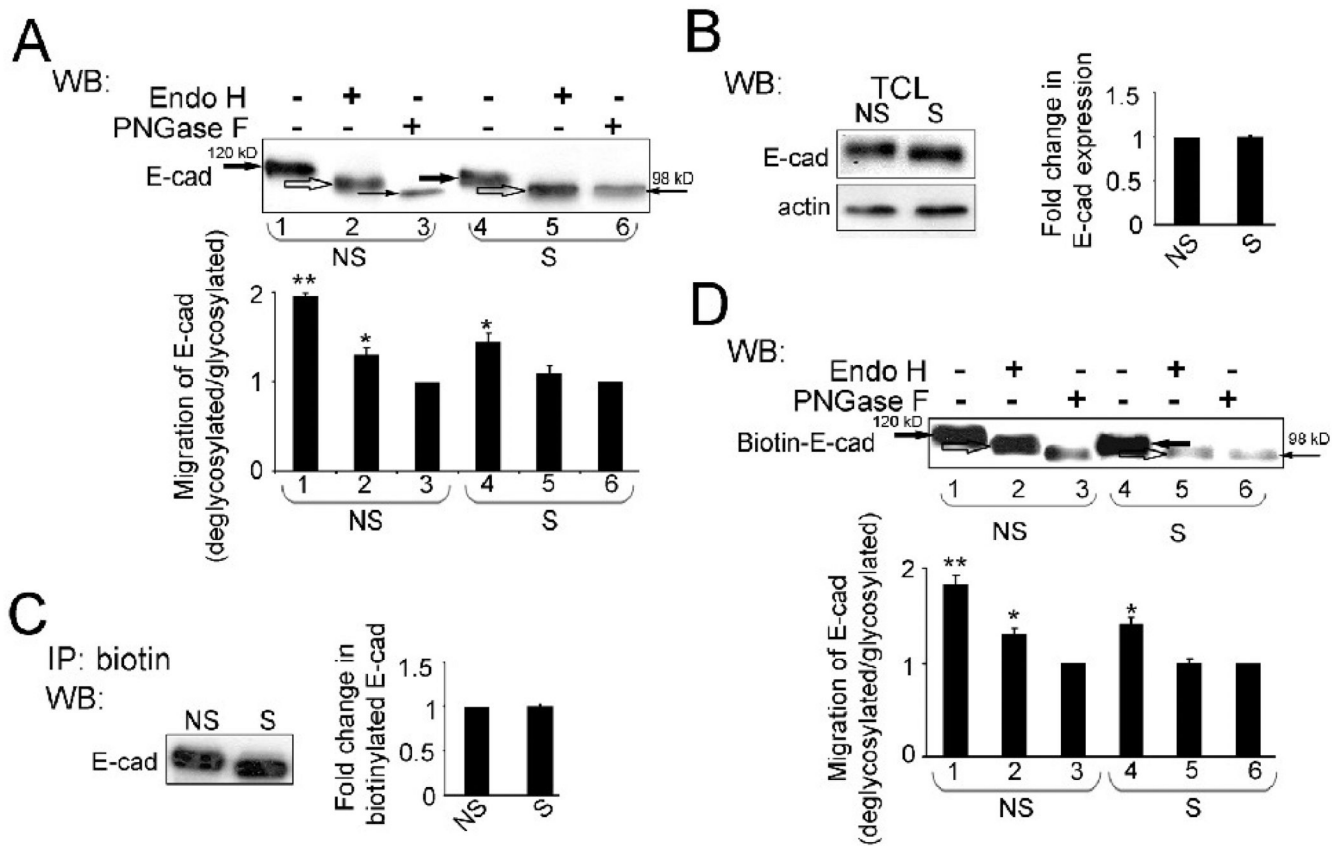
Fig. 2.
Partial inhibition of DPAGT1 reduces N-glycosylation of surface E-cadherin in MDCK cells.
(A), TCLs from non-silenced (NS) and silenced (S) cultures were treated with either EndoH
(H) or PNGaseF (F) and analyzed using WB. Results depict one of three independent
experiments (*$P<0.02$; **$P<0.01$). (B), Equal amounts of protein from non-silenced (NS) and
silenced (S) cells were analyzed for E-cadherin expression by WB. Fold change of E-cadherin
protein levels in silenced (S) cells was determined in comparison with non-silenced (NS) cells
after normalization to actin in three independent experiments. (C), non-silenced (NS) and
silenced (S) cells were biotinylated and equal amounts of biotin immunoprecipitates were
analyzed for E-cadherin expression by WB. Fold change in biotinylated E-cadherin abundance
from silenced (S) cells was determined in comparison with non-silenced (NS) cells using data
from three independent experiments. (D), Biotinylated proteins from non-silenced (NS) and
silenced (S) cells were treated with EndoH and PNGaseF and analyzed by WB. The results
depict one of three independent experiments (*$P<0.02$; **$P<0.01$).
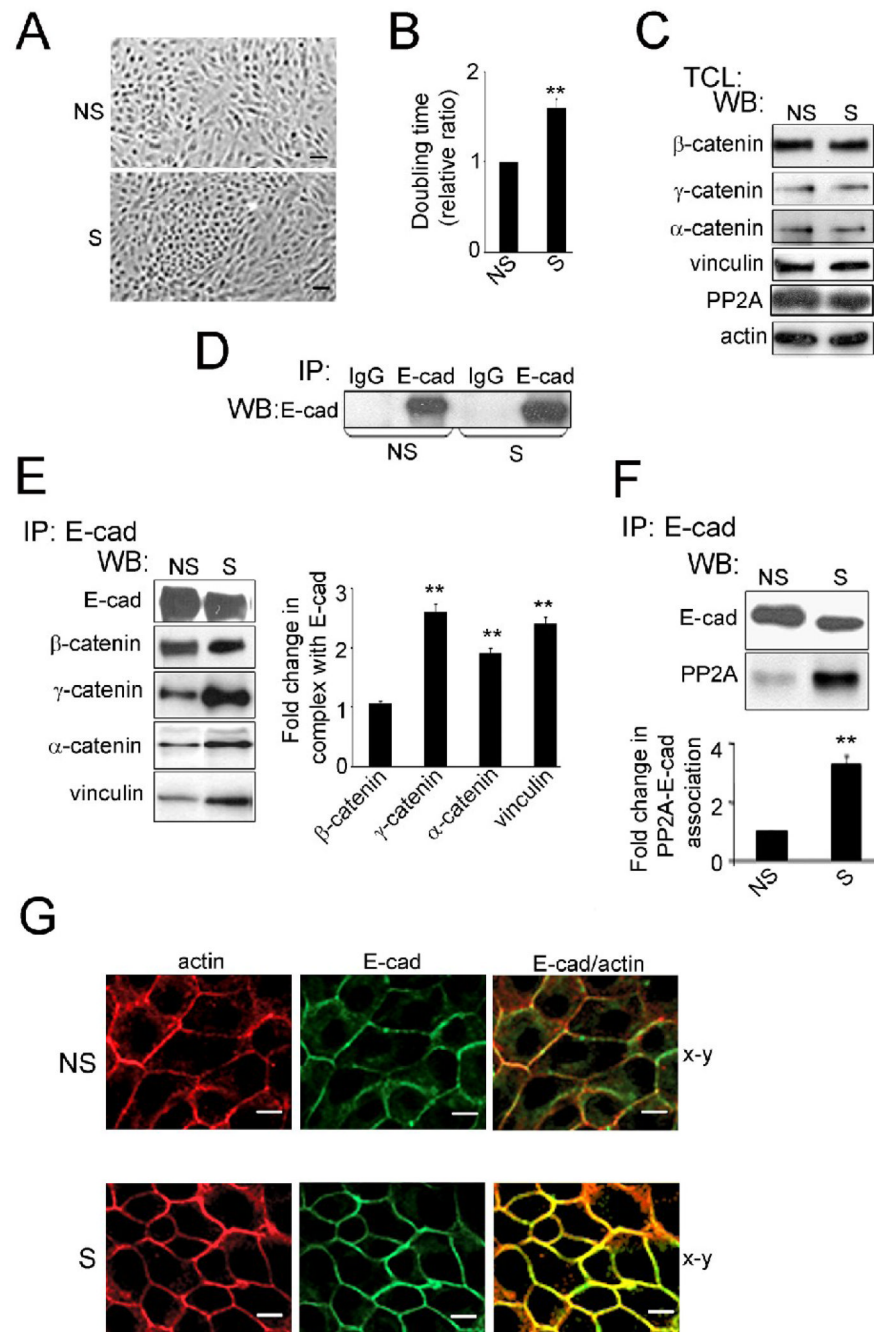
Fig. 3.
Partial silencing of DPAGT1 enhances AJs in MDCK cells. (A), Phase-contrast images of non-silenced (NS) and silenced (S) cells. Size bars, 25 µm. (B), Doubling times of non-silenced (NS) and silenced (S) cells. (**$P<0.01$). (C), TCLs from non-silenced (NS) and silenced (S) cells were examined for different catenins, vinculin and PP2A in comparison to actin by WB using data from four independent experiments. (D), Controls for immunoprecipitation experiments. TCLs were immunoprecipitated with antibodies against IgG isotypes and analyzed for expression of selected proteins by WB. (E), E-cadherins were immunoprecipitated from non-silenced (NS) and silenced (S) cells and analyzed for association with β-catenin, γ-catenin, α-catenin and vinculin by WB. Fold changes in protein levels associated with E-

cadherin complexes from silenced (S) cells were determined in comparison to E-cadherin complexes from non-silenced (NS) cells after normalization to E-cadherin abundance with data from three independent experiments (**P<0.01). (F) E-cadherins were immunoprecipitated from TCL of non-silenced (NS) or silenced (S) cells, and their association with PP2A was assessed by WB. Fold change of PP2A protein levels from silenced (S) cells was determined in comparison with non-silenced (NS) cells after normalization to E-cadherin using data from three independent experiments (**P<0.01). (G) Non-silenced (NS) or silenced (S) cells were grown to confluence and processed for indirect immunofluorescence staining using an antibody to the cytoplasmic region of E-cadherin. Cells were counterstained for F-actin with rhodamine-phalloidin. Shown are 0.74 µm confocal x-y sections. Enhanced lateral colocalization of E-cadherin and F-actin in S cells compared to NS is highlighted in x–z sections. Size bars, 10 µm.
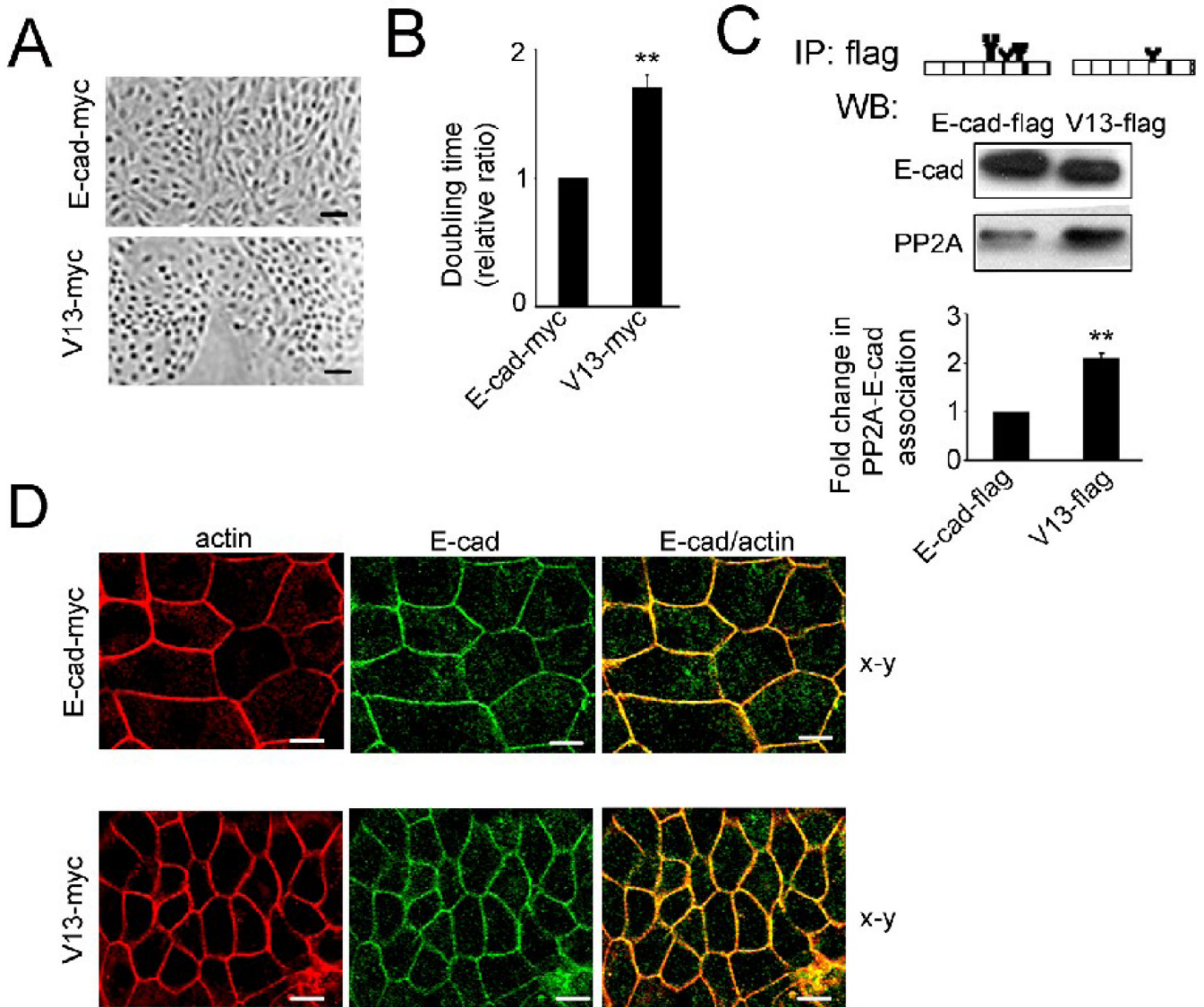
Fig. 4.
Hypoglycosylated E-cadherin enhances intercellular adhesion in MDCK cells. (A), Phase-contrast images of cells transfected with either wild type E-cadherin (E-cad-myc) or V13 (V13-myc). Size bars, 25 µm. (B), Doubling time of MDCK cells transfected with E-cad-myc and V13-myc. (**P<0.01). (C), Exogenous E-cadherins were immunoprecipitated from MDCK cells transfected with either wild type E-cadherin (E-cad-flag) or V13 (V13-flag) and examined for association with PP2A by WB. Fold change of PP2A protein level from V13-flag-transfected cells was determined in comparison with E-cad-flag-transfected cells after normalization to E-cadherin in three different experiments (**P<0.01). (D), Cells, transfected with E-cad-myc and V13-myc, were cultured in the presence of G418 to enrich for exogenous E-cadherins. Cells were immunostained for exogenous E-cadherins using an antibody to the myc tag, counterstained for F-actin with rhodamine phalloidin and examined by confocal microscopy. The images reflect 60% of cells expressing exogenous E-cadherin from a total population of 5×10^5 cells. Shown are 0.74 µm thick confocal x-y sections. Size bars, 10 µm. The images represent one of three independent experiments.
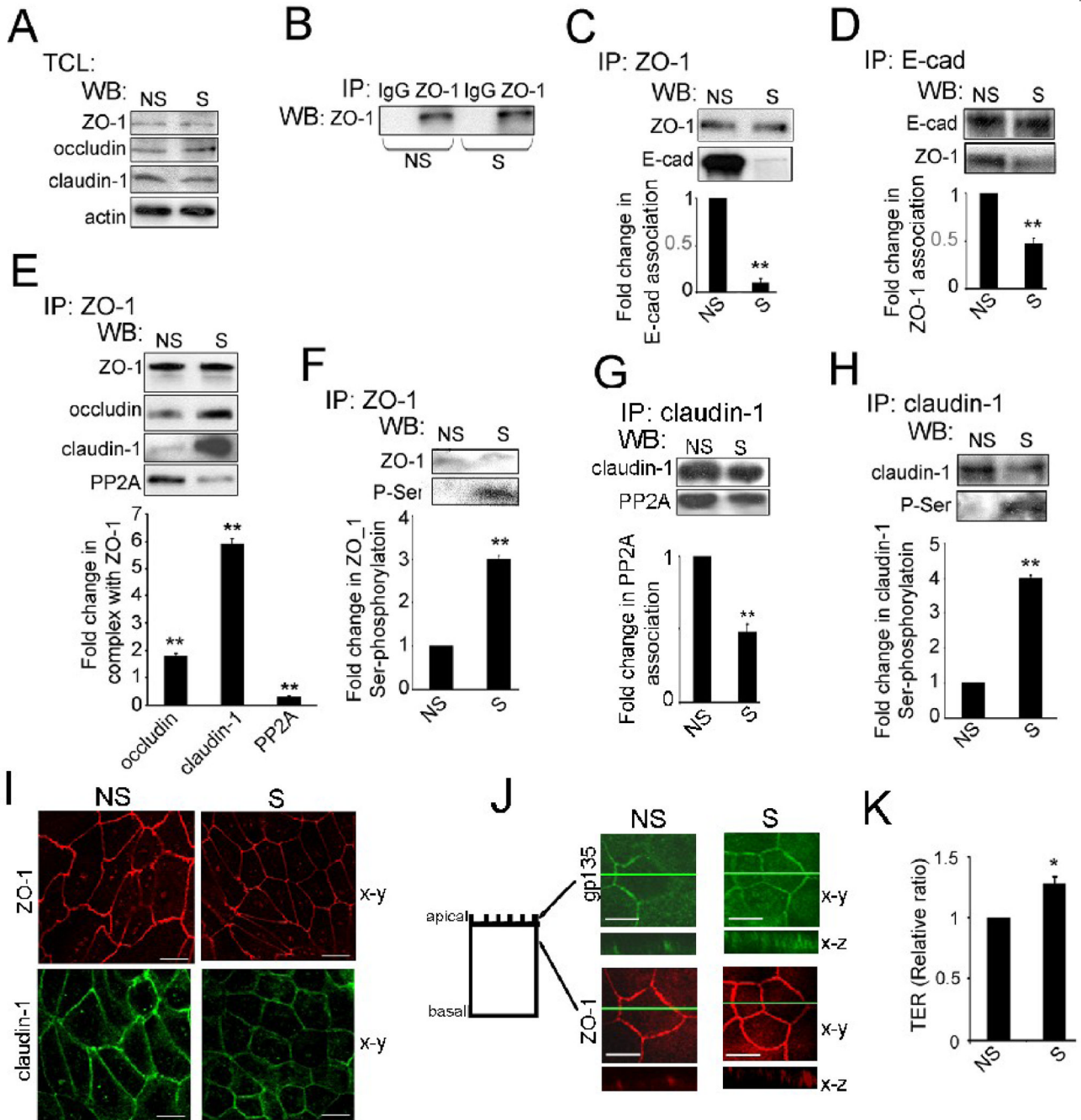
Fig. 5.
Partial inhibition of DPAGT1 promotes the assembly of TJs in MDCK cells. (A), TCLs from non-silenced (NS) and silenced (S) cells were examined for ZO-1, occludin and claudin expression by WB and compared to actin using data from four independent experiments. (B), Controls for immunoprecipitation experiments. TCLs were immunoprecipitated with antibodies against IgG isotypes and analyzed for expression of selected proteins by WB. (C), ZO-1 was immunoprecipitated from non-silenced (NS) and silenced (S) cells and analyzed for association with E-cadherin by WB. Fold change in E-cadherin levels associated with ZO-1 complexes from silenced (S) cells was determined in comparison to non-silenced (NS) cells after normalization to ZO-1 abundance using data from three independent experiments

(**P<0.01). (D), Reverse immunoprecipitation of E-cadherin in association with ZO-1. Fold change in ZO-1 levels associated with E-cadherin complexes from silenced (S) cells was determined in comparison to non-silenced (NS) cells after normalization to E-cadherin expression with data from three independent experiments (**P<0.01). (E), ZO-1 was immunoprecipitated from non-silenced (NS) or silenced (S) cells and examined for association with occludin, claudin-1 and PP2A by WB. Fold changes in the abundance of ZO-1-associated proteins from silenced (S) cells were determined in comparison with non-silenced (NS) cells after normalization to ZO-1 using data from three different experiments (**P<0.01). (F), Fold changes in ZO-1 Ser-phosphorylation levels from silenced (S) cells were determined in comparison to non-silenced (NS) cells after normalization to ZO-1 with data from three different experiments (**P<0.01). (G), Fold changes in the abundance of claudin-1-associated PP2A from silenced (S) cells were determined in comparison with non-silenced (NS) cells after normalization to claudin-1 using results from three different experiments (**P<0.01). (H), Fold changes in claudin-1 Ser-phosphorylation levels from silenced (S) cells were determined in comparison with non-silenced (NS) cells after normalization to claudin-1 with data from three different experiments (**P<0.01). (I), Immunofluorescence localization of ZO-1 and claudin-1 in non-silenced (NS) and silenced (S) cells. Shown are 0.74 µm thick confocal x-y sections. Size bars, 10 µm. Images represent one of three independent experiments. (J), Immunofluorescence localization of gp135 and ZO-1 in non-silenced (NS) and silenced (S) cells. Shown are 0.74 µm thick confocal x-y sections, with x–z sections at indicated x-y positions (green line). Size bars, 10 µm. Images represent one of three independent experiments. (K), TER measurements were carried out with confluent monolayers with duplicate samples for each siRNA. The value of TER for non-silenced (NS) cells was defined as 1.0. The results were obtained from three independent experiments (*P < 0.02).
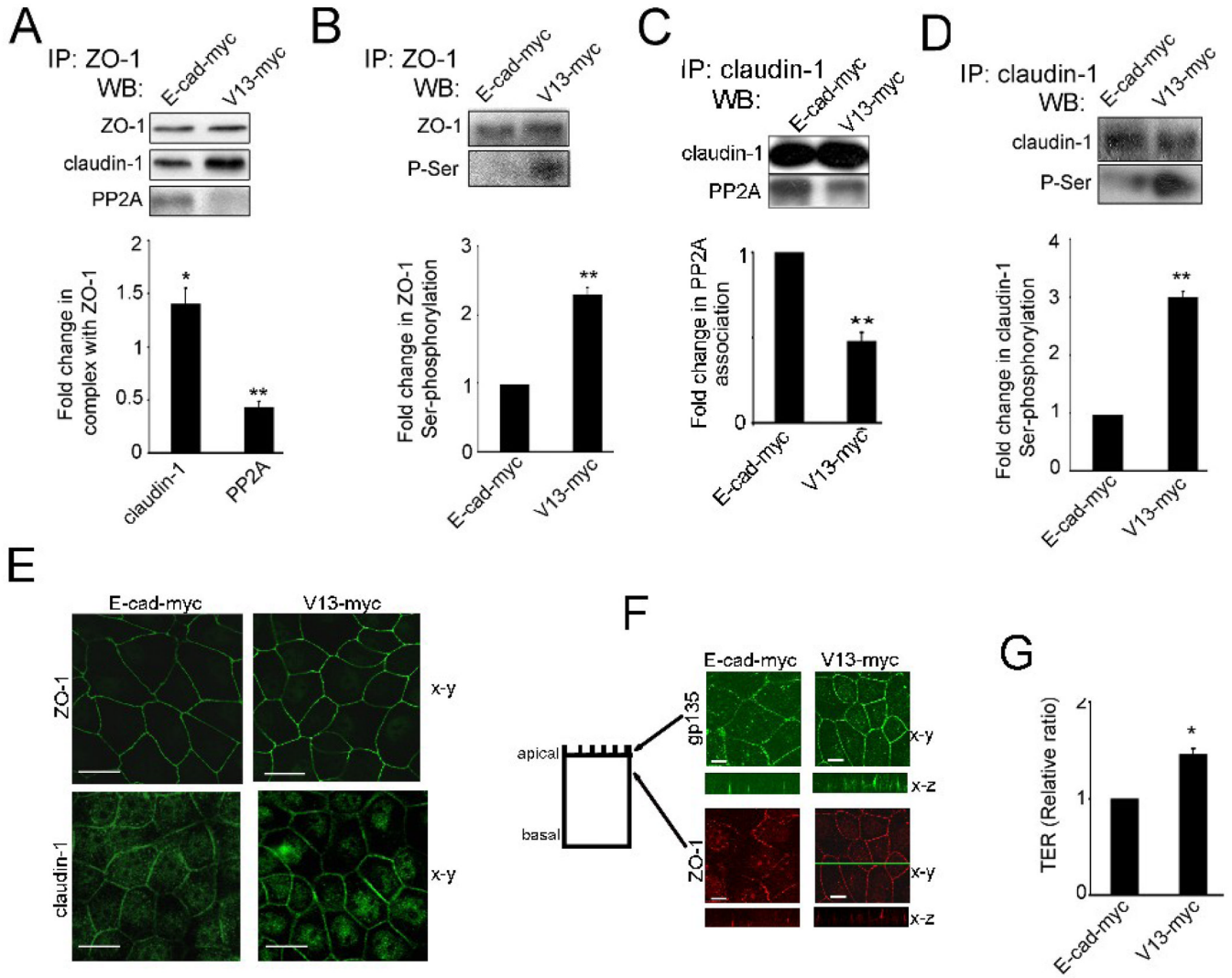
Fig. 6.
Hypoglycosylated E-cadherin drives the assembly of TJs. (A), ZO-1 was immunoprecipitated from cells transfected with either wild type E-cadherin (E-cad-myc) or V13 (V13-myc), and examined for association with claudin-1 and PP2A by WB. Fold changes in claudin-1 and PP2A levels in complex with ZO-1 in V13-myc-transfected cells were determined in comparison with E-cad-myc-transfected cells after normalization to ZO-1, based on data from three different experiments (*$P<0.02$;**$P<0.01$). (B), Fold changes in ZO-1 Ser-phosphorylation levels from V13-myc transfected cells were determined in comparison with E-cad-myc cells after normalization to ZO-1, using data from three different experiments (**$P<0.01$). (C), Fold changes in PP2A levels in complex with claudin-1 in V13 transfectants were determined in comparison with E-cad transfectants after normalization toclaudin-1, based on data from three different experiments (**$P<0.01$). (D), Fold changes in claudin-1 Ser-phosphorylation levels from V13-myc transfected cells were determined in comparison with E-cad-myc transfected cells after normalization to claudin-1 with data from three different experiments (**$P<0.01$). (E), Immunofluorescence localization of ZO-1 and claudin-1. Shown are 0.74 µm thick confocal x-y sections. Size bars, 10 µm. Images represent one of three independent experiments. (F), Immunofluorescence localization of gp135 and ZO-1 in E-cad and V13 transfectants. Shown are 0.74 µm thick confocal x-y sections, with x–z sections at

indicated x-y positions (green line). Size bars, 10 µm. Images represent one of three independent experiments. (G), TER was measured in confluent monolayers of E-cad-myc and V13-myc transfected cells, with the value for TER from E-cad-myc cells defined as 1. Data were obtained using duplicate samples from four different experiments (*$P < 0.02$).
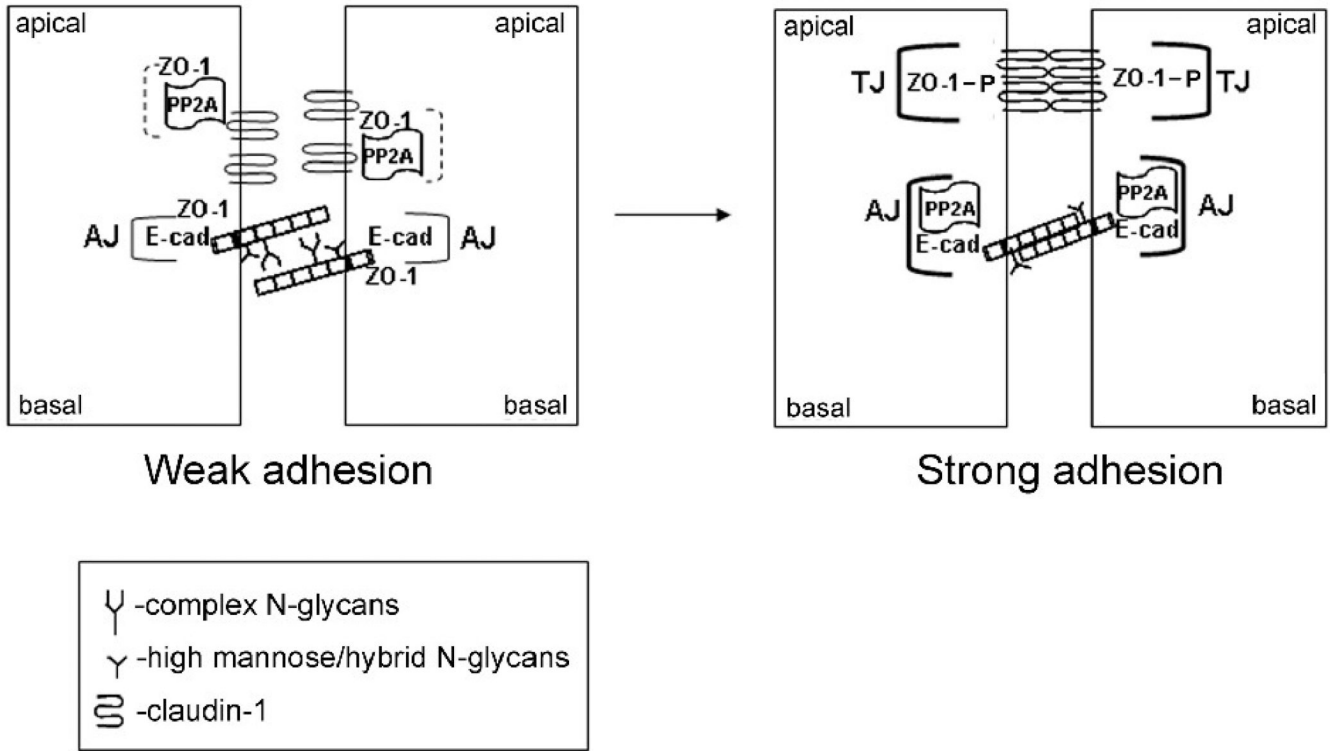
Fig. 7.
Schematic representation of how downregulation of E-cadherin N-glycosylation drives intercellular adhesion through PP2A. E-cadherin N-glycans interfere with the recruitment of PP2A to AJs, thus facilitating the association of PP2A with ZO-1 and claudin-1 (dashed brackets). Partial inhibition of E-cadherin N-glycosylation, via either siRNA to DPAGT1 or through the deletion of E-cadherin's two major N-glycan addition sites, stabilizes AJs and enhances their interaction with PP2A (bold brackets). This relieves PP2A-mediated inhibition of ZO-1 and claudin-1 phosphorylation, promotes redistribution of ZO-1 to the sites of TJs and drives TJ assembly.

Table 1

Cell cycle distribution after partial inhibition of cellular and E-cadherin-specific N-glycosylation

Sample	%G1[*]	%S + G2[*]
NS	67 +/− 2	33 +/− 2
S	78 +/− 3	22 +/−1
E-cad	87 +/− 3	13 +/−1
V13	93 +/− 2	7 +/−1

[*]
% total cells gated